The background is a solid purple color with several abstract geometric elements. A large, semi-transparent circular graphic is centered on the right side, featuring concentric rings and a dotted border. Diagonal lines and a grid of small dots are also visible in the lower-left quadrant.

III-5

Life, Earth and
Planetary Sciences

BL4U

Drug Release and Probing of Thermoresponsive Nanogels in Human Skin by Soft X-Ray Spectromicroscopy

K. Yamamoto¹, A. Klossek¹, T. Ohigashi², F. Rancan³, R. Flesch¹, M. Giubudagian¹, A. Vogt³, U. Blume-Peytavi³, P. Schrade⁴, S. Bachmann⁴, M. Calderón¹, M. Schäfer-Korting⁵, N. Kosugi² and E. Rühl¹

¹Institute for Chemistry and Biochemistry, Freie Universität Berlin, Takustr. 3, 14195 Berlin, Germany

²UVSOR Synchrotron Facility, Institute for Molecular Science, Okazaki 444-8585, Japan

³Charité Universitätsmedizin, 10117 Berlin, Germany

⁴Abteilung für Elektronenmikroskopie at CVK, 13353 Berlin, Germany

⁵Institut für Pharmazie, Freie Universität Berlin, 14195 Berlin, Germany

The transport of drugs into human skin facilitated by triggered drug release from polymeric nanocarriers is reported. Label-free detection by X-ray microscopy is used to probe both, the drug and the drug nanocarriers. Dexamethasone (DXM) is used as a drug and the thermoresponsive gel was Poly(N- isopropylacrylamide) (nanogel). The stratum corneum (SC) is the top skin layer. It is the main barrier, which hinders drugs to penetrate into the viable epidermis. We recently published first results using X-ray microscopy for selectively probing DXM [1, 2] and core-multishell nanocarriers penetrating human skin [3]. It was shown that nanocarriers release the drug in the SC without penetrating into deeper skin layers. This yields higher local drug concentrations in the viable epidermis than for conventional drug formulations [3].

The experiments made use of excised human skin, which was exposed to DXM-loaded nanogels for penetration times of 100 and 1000 min. The nanogels were dissolved in water with a concentration of 33.5 mg/mL and had a drug load of 10%. Excised human skin was tape-stripped 30 times prior to topical drug application. In total 120 μ L of this nanogel suspension containing 400 μ g of DXM was applied per cm^2 of skin. Triggered drug release was initiated after 10 min by exposure of the skin samples to infrared radiation for 30 s, leading to a contraction of the nanogel and drug release.

Spectromicroscopy studies were performed at the BL4U beamline at UVSOR III using a scanning X-ray microscope. The chemical selectivity for probing either the thermoresponsive nanogel or DXM in fixed skin was achieved by exciting the samples selectively at the oxygen K-edge in the pre-edge regime (cf. [1-3]). Differential absorption maps were derived, similar to our previous work (see Fig. 1).

Figure 1 shows a compilation of the results, where only the top skin layers are shown (SC and top part of the viable epidermis). Fig. 1 (a) - (d) show results for the nanogel distribution, whereas Fig. 1 (e) - (h) show the drug distribution. Triggered and non-triggered conditions result in distinct differences for both, the drug and the drug nanocarrier distributions. The nanogel appears to penetrate only efficiently the SC, if triggered by IR radiation (Fig. 1 (b), (d)), but cannot reach the viable epidermis. Moreover, significant drug

release and penetration into deeper layers only occurs, if the release is thermally triggered (Fig. 1 (f), (h)). The nanogel also provides in the SC access for the drug into the corneocytes, which has not been observed before using other vehicles, then DXM remained in the lipid regions between the corneocytes [1-2]. This nanogel-induced effect goes along with swelling of the corneocytes, which has been recently observed by electron microscopy [4]. Stimulated Raman studies provide additional evidence that this is related to changes the organization of proteins and lipids [4]. These results underscore that label-free detection at high spatial resolution provides novel insights that are required for the optimization of topical drug delivery strategies facilitated by polymeric drug nanocarriers.

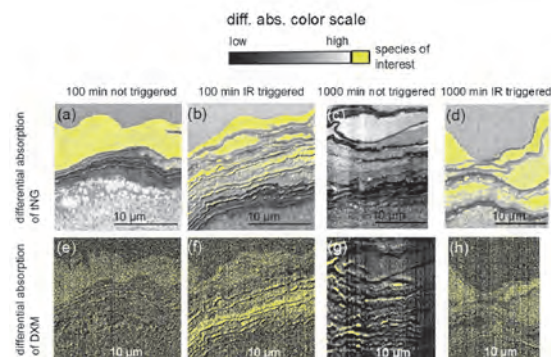


Fig. 1. The differential absorption of dexamethasone loaded nanogels penetrating the top skin layers for 100 and 1000 min, respectively: (a) - (d) selective probing of the nanogel; (e) - (h) selective probing of dexamethasone. Triggered ((b), (d), (f), (h)) and non-triggered ((a), (c), (e), (g)) drug release conditions show different distributions of the selected species.

- [1] K. Yamamoto *et al.*, *Anal. Chem.* **87** (2015) 6173.
 [2] K. Yamamoto *et al.*, *Eur. J. Pharm. Biopharm.*, in press (2017). DOI: 10.1016/j.ejpb.2016.12.005.
 [3] K. Yamamoto *et al.*, *J. Control. Release* **242** (2016) 64.
 [4] M. Giubudagian *et al.*, *J. Control. Release* **243** (2016) 323.

BL1U

Optical Activity Emergence in Glycine by Circularly Polarized Light

J. Takahashi^{1,2}, N. Suzuki¹, Y. Kebukawa¹, K. Kobayashi¹, Y. Izumi³, K. Matsuo³,
M. Fujimoto⁴ and M. Katoh⁴

¹*Faculty of Engineering, Yokohama National University, Yokohama 250-8501, Japan*

²*Institute of Laser Engineering, Osaka University, Suita 565-0871, Japan*

³*Hiroshima Synchrotron Radiation Center, Higashi-Hiroshima 739-0046, Japan*

⁴*UVSOR Facility, Institute for Molecular Science, Okazaki 444-8585, Japan*

The origin of homochirality in terrestrial bioorganic compounds (L-amino acid and D-sugar dominant) is one of the most mysterious issues that remain unresolved in the study of the origin of life. Because bioorganic compounds synthesized in abiotic circumstances are intrinsically racemic mixtures of equal amounts of L- and D-bodies, it is hypothesized that chiral products originated from asymmetric chemical reactions induced by a “chiral impulse”. These types of asymmetric reactions could have possibly been derived from physically asymmetric excitation sources in space and the chiral products would have been transported to primitive Earth resulting in terrestrial homochirality (Cosmic Scenario) [1]. In space, asymmetric excitation would be mainly effectuated by polarized photons of synchrotron radiation (SR) from kinetic electrons captured by strong magnetic field around neutron stars or white dwarfs in supernova explosion area, or by polarized photons scattered by interstellar dust clouds in star formation areas. Eventually, several terrestrial observations of polarized photon radiation from space due to scattering by interstellar dust clouds in star formation regions have been reported [2].

Several experiments have already examined asymmetric photochemical reactions in simple biochemical molecules by using circularly polarized light (CPL). We have reported optical activity emergence in solid-phase films of racemic mixtures of amino acids by using CPL from UVSOR-II free electron laser (FEL) [3].

In this paper, optical activity emergence into the achiral (optically inactive) amino acid film by using CPL is reported. We formed thin solid films of glycine on fused quartz substrates from crystal powders of glycine using a thermal-crucible vacuum evaporator. Sublimation temperature was 150 ~ 200 °C and pressure of the vacuum chamber was approximately 10⁻² Pa throughout the evaporation process. To introduce optical asymmetry into the racemic film, we irradiate them with CPL introduced from undulator beam line BL1U of UVSOR-III (Fig.1). The irradiated CPL wavelength was 215 nm and total irradiation energies were 12 and 20 mW hour.

In order to clarify the optical anisotropy of the films, we measured the circular dichroism (CD) and photo absorption spectra using a commercial CD

spectrometer (JASCO J-720WI). As a result, almost completely symmetric spectra were observed with left- and right-handed CPL irradiation. The dependence on sample rotation angle of the spectra of 0- and 90-degree rotation was measured. If linear dichroism (LD) and/or linear birefringence (LB) components are dominantly effective, the signs of appearance CD peaks should be inverted. We ensured that rough spectrum profile and at least signs of two CD peaks were not changed. Therefore, observed appearance CD should be derived dominantly from chiral CD component. We are planning CD spectra measurement over the shorter wavelength region using SR-CD beamline of Hiroshima Synchrotron Radiation Center (HiSOR).

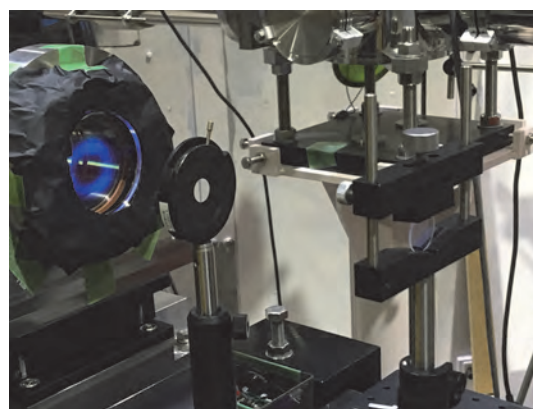


Fig. 1. Photo of the irradiation experiment of circularly polarized light on BL1U.

- [1] Bonner, *Origins Life Evol. Biosphere* **21** (1991) 59.
 [2] T. Fukue *et al.*, *Origins Life Evol. Biosphere* **40** (2010) 335.
 [3] J. Takahashi, H. Shinojima, M. Seyama, Y. Ueno, T. Kaneko, K. Kobayashi, H. Mita, M. Adachi, M. Hosaka and M. Katoh, *Int. J. Mol. Sci.* **10** (2009) 3044.

BL1U

Emergence of Biological Homochirality by Irradiation of Polarized Quantum Beams

K. Matsuo¹, Y. Izumi¹, J. Takahashi², M. Fujimoto³ and M. Katoh³

¹Hiroshima Synchrotron Radiation Center, Hiroshima University, Higashi-Hiroshima 739-0046, Japan

²Faculty of Engineering, Yokohama National University, Yokohama 240-8501, Japan

³UVSOR Facility, Institute for Molecular Science, Okazaki 444-8585, Japan

Origin of homochirality in terrestrial biomolecules (L-amino acids and D-sugars dominant) remains an unresolved problem. One of the hypotheses for the emergence of homochirality is Cosmic Scenario, in which the space materials on the surface of meteorites are transformed into the complex organic molecules (for example amino acid precursors) by the asymmetric reactions due to the irradiation of circularly polarized light (CPL). To validate this scenario, as a pioneer research, Takahashi et al. investigated the emergence of optical anisotropy in solid films of racemic amino acids (L/D = 1) with the left- and right-CPL (LCPL and RCPL) irradiation of 215 nm, and suggested that the CPL caused the preferential conformational changes between the two enantiomers in racemic amino acid films [1].

Circular dichroism (CD) spectroscopy can easily detect the emergence of optical anisotropy due to the asymmetric reaction because it sensitively reflects the steric structures of chiral molecules such as amino acids. Further the theoretical calculation of CD spectrum of L-alanine molecule revealed that the chromophores such as carboxyl and amino groups had many characteristic electronic transitions ($n-\pi^*$, $\pi-\pi^*$ and $n-\sigma^*$) below 230 nm [2], suggesting that the photoreaction might depend on the irradiation energy. In this study, the thin solid films of racemic alanine (L/D = 1) were irradiated by the two types of CPL wavelengths (230 and 202 nm) and the emergence of amino acid homochirality were investigated by the CD measurements.

The thin solid films on SiO₂ substrates were produced by evaporating the powder of DL-alanine using the vacuum-evaporation system in Hiroshima Synchrotron Radiation Center (HiSOR). Sublimation temperature was about 150 ~ 200 °C and the pressure in the vacuum chamber during the evaporation was approximately 5×10^{-2} Pa. The CD spectra of these thin solid films were measured from 260 to 170 nm using a vacuum-ultraviolet circular dichroism instrument in HiSOR and confirmed to be mostly zero before the irradiation, showing that the spurious CD due to the contamination of film surface were negligible. The LCPL and RCPL irradiation for these films were carried out in the BL1U of UVSOR at the wavelengths of 230 and 202 nm. After the irradiation, these CD spectra were measured again, in order to confirm the emergence of homochirality.

Figure 1 shows the CD spectra of thin films after the

LCPL and RCPL irradiation of two wavelengths. As shown in Fig. 1, the LCPL and RCPL irradiation exhibited symmetrically inverted spectra in the both irradiation wavelengths (230 and 202 nm), indicating the emergence of homochirality at the both irradiation wavelengths. Further, the spectral shape observed in Fig.1a were largely different from those in Fig.1b, suggesting that the asymmetric reactions of DL-alanine thin solid film depend on the irradiation wavelength.

To further validate these results, we are planning to irradiate the CPL in the vacuum-ultraviolet region. Accumulations of these experimental results would be useful for determining the effective emergence of homochirality in solids by the CPL irradiation.

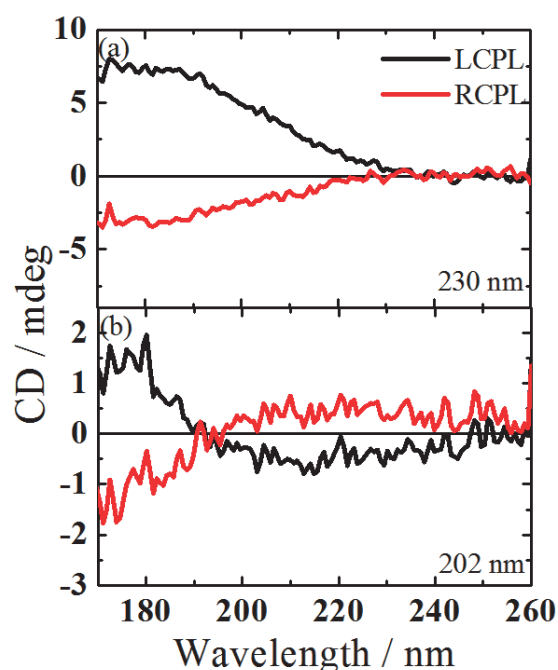


Fig. 1. CD spectra of DL-alanine thin films after the LCPL and RCPL irradiation at 230 nm (a) and 202 nm (b).

- [1] J. Takahashi, H. Shinjima, M. Seyama, Y. Ueno, T. Kaneko, K. Kobayashi, H. Mita, M. Adachi, M. Hosaka and M. Katoh, *Int. J. Mol. Sci.* **10** (2009) 3044.
 [2] T. Fukuyama, K. Matsuo and K. Gekko, *J. Phys. Chem. A* **109** (2005) 6928.

BL4U

STXM Study on the Microbial Alteration of Iron Sulfide Mineral at the Submarine Seafloor

S. Mitsunobu^{1,2}, Y. Ohashi² and T. Ohigashi³¹Department of Agriculture, Ehime University, Matsuyama 790-8566, Japan²Institute for Environmental Sciences, University of Shizuoka, Shizuoka 422-8526, Japan³UVSOR Facility, Institute for Molecular Science, Okazaki 444-8585, Japan

Recent studies have revealed that various microorganisms are alive on the submarine seafloor and contribute alteration of oceanic crust [1, 2]. It is considered that the microorganisms (e.g., bacteria, archaea) gain their life-energy from the redox reaction using inorganic active elements such as ferrous iron and sulfur involved in the oceanic crust (basaltic rocks and sulfidic minerals). The microbial activities would accelerate the alteration of the oceanic crust, which would influence the carbon dynamics in the earth significantly. However, little is known on mechanism of the microbial alteration of the minerals, because direct chemical speciation of both metals and biomolecules at mineral-microbe interface has been crucial due to high spatial resolution in analysis. Moreover, difficulty on the field access is also an obligate reason that no enough studies on that has been done so far.

Here, we performed *in situ* bio-alteration experiment using mineral substrates composed of the ocean crust, fresh sulfidic mineral (pyrite) and basalt rock, at oxidative submarine seafloor in Izu-Bonin region, where oxidative alteration of the basalt and pyrite naturally occur. Then, we investigated the mechanisms of the bio-alteration process using scanning transmission X-ray microscopy (STXM) based C and Fe near edge X-ray absorption fine structure (NEXAFS) analyses at UVSOR BL4U.

Before STXM analysis, bacteria attached on the pyrite were stained with a minimum fluorescent dye and marked for the STXM analysis. In the analysis, we applied the STXM analysis to determine *in situ* carbon (C) and iron (Fe) species at the interface of target bacteria cell and mineral (pyrite). STXM-based imaging and C 1s NEXAFS analysis directly showed that the attached bacterial cell produce some polysaccharide-rich extracellular polymeric substances (EPS) at the cell-pyrite interface (data not shown). The polysaccharide substances generally have a metal-chelating effect and enhance the dissolution of mineral involving the metals [3]. Hence, the bacteria may produce the polysaccharide-rich EPS on the pyrite actively to dissolve the pyrite and gain energy efficiently.

Furthermore, we measured STXM-based Fe imaging and Fe 4p NEXAFS at the same area. Figure 1 (a) shows the STXM-based merged Fe/C image. The image shows the several particles yielding Fe with diameter of 50-100 nm on the cells (orange circles in Fig. 1 (a)). The Fe NEXAFS analysis of the particles

indicate that Fe species in these particles were Fe(III) hydroxides such as ferrihydrite and schwertmannite on the whole (Fig. 1 (b)). Because the Fe species in substrate (pyrite) is Fe(II), observed Fe(III) results from oxidation of Fe(II) originally involved in pyrite. These findings indicate that some of bacteria attached on the pyrite gain energy by Fe oxidation at the submarine seafloor and that have a metabolic mechanism to excrete subsequent insoluble-Fe(III) formed by oxidizing reaction.

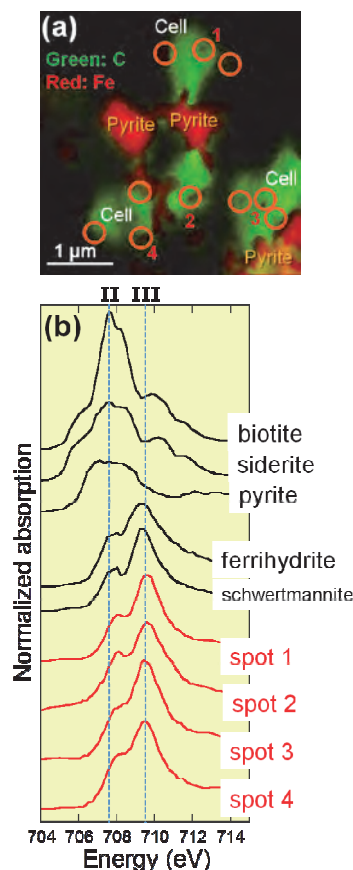


Fig. 1. STXM-based C and Fe images (a) and Fe 4p NEXAFS spectra (b).

- [1] T. M. McCollom, *Deep-Sea Res.* **47** (2000) 85.
 [2] K. J. Edwards *et al.*, *Geochim. Cosmochim. Acta* **67** (2003) 2843.
 [3] S. Mitsunobu *et al.*, *Microbes Environ.* **31** (2016) 63.

BL4U

NEXAFS Measurements of Biomolecules at the C-K edge for Molecular Mapping in Biological Specimens by STXM

A. Ito¹, T. Ohigashi^{2,3}, K. Shinohara¹, S. Tone⁴, M. Kado⁵, Y. Inagaki² and N. Kosugi^{2,3}

¹School of Engineering, Tokai University, Hiratsuka 259-1292, Japan

²UVSOR Synchrotron, Institute for Molecular Science, Okazaki 444-8585, Japan

³The Graduate University for Advanced Studies (SOKENDAI), Okazaki 444-8585, Japan

⁴Graduate School of Science & Engineering, Tokyo Denki University, Hatoyama 350-0394, Japan

⁵Kansai Photon Science Institute, Nat. Inst. Quantum and Radiological Sci. Technol., Kizugawa 619-0215, Japan

Spectromicroscopy using scanning transmission X-ray microscope (STXM) has been applied to DNA and protein distributions in biological specimens such as chromosome and sperm at the C-K absorption edge [1, 2]. In our previous studies using STXM at BL4U, we obtained DNA and histone, a nuclear protein, distributions in mammalian cells using characteristic NEXAFS peaks of DNA and histone which can be clearly observed at the N-K absorption edge [3]. Furthermore quantitative mapping of these molecules was developed [4], but the results showed that the contribution of biomolecules other than DNA and histone should be taken into account.

In this study we measured NEXAFS of phospholipids, a major component of cellular membrane, in addition to nucleic acids and various kinds of proteins at the C-K absorption edge. Figure 1 shows NEXAFS for typical biomolecules of nucleic acid, protein and phospholipid at the C-K absorption edge.

Ade *et al.* used the slight shift of a peak as shown by 1 and 2, which was assigned to 1s to π^* transition of C=C bond, to image of DNA and protein in chromosome separately [1]. The significant difference in peaks among nucleic acid, protein and phospholipid can be observed at the peak 6, 7 and 8 as indicated in Fig. 1. These peaks were assigned to 1s to π^* transition of C=O bond [5, 6]. Peak 6 and 8 corresponds to N-C(=O)-C and N-C(=O)-N, respectively. On the other hand phospholipid does not have such amide bonds, but has O-C=O. This bond may result in the unique peak 7. The different location of peaks due to C=O bond may be applicable to separate imaging of these molecules.

Figure 2 shows the comparison of DNA and RNA in the NEXAFS at the C-K edge. Peaks 5 and 6, 1s to π^* transition of C=O bond, exhibits a slight difference, suggesting the possibility for imaging nucleic acids separately.

For the difference among proteins, we measured spectra of bovine serum albumin (BSA), histone, cytochrome C and actin. NEXAFS peaks have the same energies except actin. Interestingly actin has the significant peak shift to higher energies. This finding needs to be confirmed in future experiments.

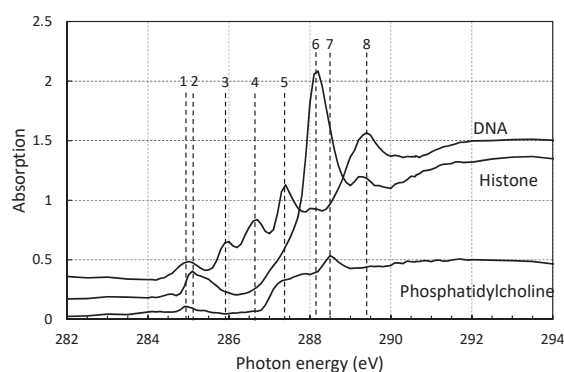


Fig. 1. NEXAFS spectra of DNA, histone and phosphatidylcholine at the C-K absorption edge.

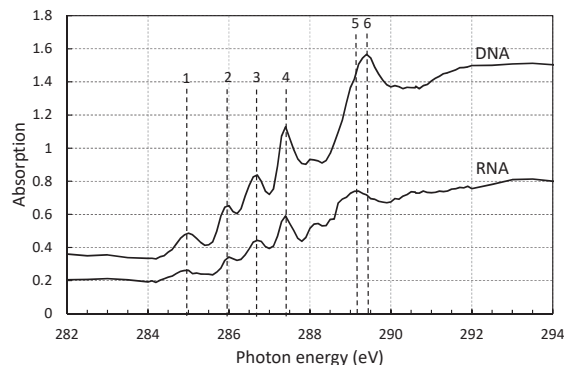


Fig. 2. NEXAFS spectra of DNA and RNA at the C-K absorption edge.

- [1] H. Ade *et al.*, Science **258** (1992) 972.
- [2] X. Zhang *et al.*, J. Struct. Biol. **116** (1996) 335.
- [3] A. Ito, T. Ohigashi, K. Shinohara, S. Tone, M. Kado, Y. Inagaki and N. Kosugi, UVSOR Activity Report **43** (2016) 143.
- [4] K. Shinohara, T. Ohigashi, S. Tone, M. Kado and A. Ito, Proc. 13th Intl. Conf. X-Ray Microsc. (XRM2016) (in press).
- [5] Kummer *et al.*, J. Phys. Chem. B **114** (2010) 9645.
- [6] Stewart-Ornstein *et al.*, J. Phys. Chem. B **111** (2007) 7691.

BL4U

Chemical Speciation of Single Aerosol Particles: A Reconstruction of Hygroscopicity for Sulfate Aerosols

Y. Takahashi¹, C. Miyamoto¹ and K. Sakata²¹Department of Earth and Planetary Science, Graduate School of Science, the Univ. of Tokyo, Tokyo 113-0033, Japan²Department of Earth and Planetary Systems Science, Graduate School of Science, Hiroshima Univ., Higashi-Hiroshima 739-8526, Japan

Hygroscopic sulfate aerosol such as ammonium sulfate (AS: $(\text{NH}_4)_2\text{SO}_4$) contributes to indirect cooling effect by acting as cloud condensation nuclei (CCN) [1]. On the other hand, gypsum (Gyp: $\text{CaSO}_4 \cdot 2\text{H}_2\text{O}$), non-hygroscopic sulfate, suppresses CCN activity of AS, which are formed by chemical reaction of calcite (Cal: CaCO_3) in mineral dust with H_2SO_4 in atmosphere [2]. Thus, non-sea-salt sulfate (nssSO_4^{2-}) species is one of the important information for estimation of CCN activity of sulfate aerosol.

Ice sheet in polar region preserves atmospheric particles and gases at the time of its deposition [3]. In the case of Greenlandic ice sheet, they preserve mineral dust and anthropogenic aerosol from continental region in the Northern hemisphere [3]. In this study, chemical speciation experiments of trapped particles in ice sheet were conducted. In addition, chemical speciation in sea spray aerosol (SSA) with high CCN activity was also conducted to distinguish non-sea-salt sulfate (nssSO_4^{2-} : AS and Gyp) and SO_4^{2-} from seawater. The aim of this study is to determine Gyp/AS ratio in trapped particles in ice sheet to estimate CCN activity of nssSO_4^{2-} aerosols in the past.

Trapped particles in Greenlandic ice sheet were extracted by sublimation of ice samples in low temperature room (-20°C), which can extract trapped particles with minimal chemical alteration by water from melting ice samples [4]. Trapped particles in ice sheet with ages of 1987, which is a part of ice core drilled at SE-Dome (67.2°N , 36.4°W , 3170 m above sea level), were analyzed. SSA sampling were conducted at the Antarctic Ocean to obtain non-alteration SSA by anthropogenic gases (*R/V Hakuho-Maru* cruise, KH-14-6, GEOTRACES). Chemical speciation experiments were conducted by STXM/NEXAFS with image stack [5].

Sulfate and Ca in SSA were enriched in edge position of aerosol particles (Fig. 1). Carbonate distribution in single SSA particles, for which we measured carbon K-edge NEXAFS, were similar between sulfate and Ca (Fig. 1). The spectral analysis showed that Ca species were aragonite (Arg: CaCO_3) and Gyp. Sulfate in SSA was also present as Na_2SO_4 , which was hygroscopic sulfate. Considering that Na and Ca concentration in SSA, Na concentrations is much higher than that of Ca. Therefore, dominant sulfate species in SSA can be Na_2SO_4 . On the other hand, center part of SSA was composed of NaCl, which result is consistent with a previous study [5]. Thus, SSA surface and center were composed of sulfate with Ca, Na and C, and NaCl,

respectively (Fig. 1).

Sulfate and Ca are distributed heterogeneously in trapped particle in Greenlandic ice sheet (Fig. 2). Distributions of sulfate and Ca in trapped particles were different from those in SSA (Figs. 1 and 2). Therefore, mineral dust and SSA can be distinguished based on distributions of sulfate and Ca. Unfortunately, AS-bearing particles cannot be detected from Greenlandic ice sheet due to the small number of measured particles. Previous studies reported that AS particle contains sulfate homogeneously in the single particle [6]. Thus, SSA, mineral dust, and AS particles can be distinguished by sulfate distributions in their single particles. Therefore, S speciation for trapped particles by STXM/NEXAFS and estimation of AS and Gyp amount of based on optical density (OD) of SO_4^{2-} lead to reconstruction of CCN activity of sulfate aerosol in the past.

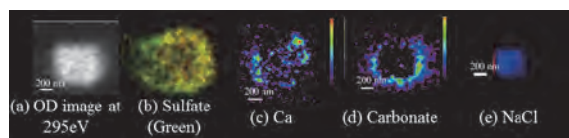


Fig. 1. Results of image stack of SSA. (a) OD image at 295 eV, (b-e) sulfate, Ca, carbonate, and NaCl distributions, respectively.

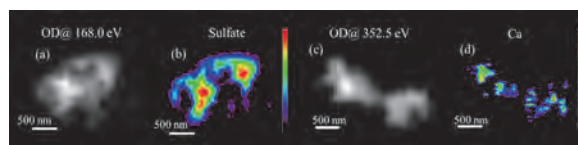


Fig. 2. Results of image stack of two trapped particles in Greenlandic ice sheet: (a) OD image at 168.0 eV, (b) sulfate distribution, (c) OD image at 352.5 eV, and (d) Ca distribution.

- [1] C. D. O'Dowd *et al.*, *Atmos. Environ.* **31** (1997) 73.
- [2] Y. Takahashi *et al.*, *Environ. Sci. Technol.* **43** (17) (2009) 6535.
- [3] R. J. Delmas, *Rev. Geophys.* **30** (1) (1992) 1.
- [4] Y. Iizuka *et al.*, *J. Glaciology* **55** (191) (2009) 552.
- [5] R. C. Moffet *et al.*, *Anal. Chem.* **82** (2010) 7906.
- [6] W. Li *et al.*, *J. Clean. Prod.* **112** (2016) 1330.

BL4U

Evaluation of Influence on Organic Matters by Dehydration of Hydrous Asteroids

A. Nakato¹ and M. Uesugi²¹ Division of Earth and Planetary Sciences, Kyoto University, Kyoto, 606-8502, Japan² SPring-8/JASRI, Sayo, 679-5198, Japan

Extraterrestrial organics in the carbonaceous chondrites show wide variety and complex structures. Those characteristics of the structure could be evidences of the evolution of the parent body since the structure would be modified due to thermal metamorphism and aqueous alteration [e.g., 1, 2]. Many previous studies have investigated the structural change of the insoluble organic matters (IOM) extracted from the meteorites, but lacked ‘*in situ*’ investigation of organics in meteorites. XANES and high resolution STXM installed in UVSOR BL4U are useful tools for such ‘*in situ*’ analysis of molecular structure of the organics in bulk rock of unknown carbonaceous chondrites, and observation of their micro- distribution. We prepared two types carbonaceous chondrites, one is Murchison that experienced aqueous alteration, and the other is Allende that was suffered thermal metamorphism on the parent body, respectively. Both samples were made by focused ion beam (FIB), and analyzed by STXM/XANES. In addition, we examined that sample contamination during the storage [3], and sample damage due to sample preparing methods [4] suggested by previous studies.

We fibbed 8 samples from the matrix of Murchison polished thick section. The size is about 15x10 μm and 100 nm thickness. An Allende fragment was embedded into sulfur and then sliced about 70 nm thick each by ultramicrotome. After that, the remaining portion was picked up from the sulfur and embedded in epoxy to be fibbed into 5x5 μm and 100 nm thickness sections. These processes of Allende were performed for comparison of the sample damage between the preparing methods. STXM and C, N, O-NEXAFS was carried out for all samples formed by FIB and ultramicrotome.

For evaluation of the sample contamination during the storage, Murchison samples were kept in 4 different conditions for 6-8 months. The storage atmospheres were pure Nitrogen and approximately 10^2 Pa vacuumed conditions. The sample holder made by Si and metal, respectively.

Several characteristic peaks of aromatic carbon at 285 eV, aliphatic carbon at 287.5 eV, carboxyl at 288.5 eV, and carbonate 290.5 eV were detected from Murchison samples as same as the previous studies of IOM [e.g., 5]. Most of the Murchison samples show similar peaks except for those of carbonate. It suggests that the molecular structure of organics in Murchison is relatively primitive and homogeneous. On the other hand, it is well known that Allende IOM

shows unique chemical structure of $1s-\sigma^*$ exciton at 291.7 eV of graphene structures, that is a characteristic of thermally metamorphosed meteorites [5]. However, we could not detect the peak in both fibbed and microtomed samples in this study (Fig. 1). It may reflect that the graphene can be concentrated in extracted sample, or apparently masked by features of other organic components in *in situ* observation of bulk sample. In other words, we found fine-scaled heterogeneity of organic matter in Allende matrix using XANES and high resolution STXM, though further investigation is required. C-XANES of Murchison and Allende did not show any differences of the organic molecular structures. Thus, any influences on the organic matter by thermal metamorphism were not found in our ‘*in situ*’ bulk analysis and observation so far.

C-XANES spectrum of Murchison samples stored for 6-8 months do not show any changes irrespective of the storage environment. In addition, we can not detect clear N-XANES transition in all samples, even some samples were kept in pure N_2 atmosphere. We can conclude from these results that sample storage does not give any contaminations, under the conditions tested in our study.

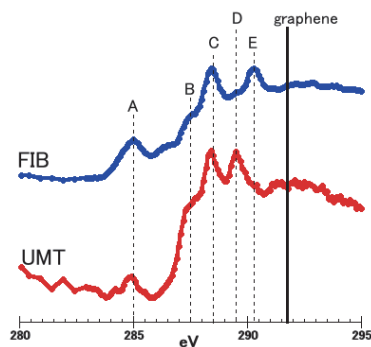


Fig. 1. C-XANES spectra of Allende.

Peaks indicated with letters A-E. A: aromatic carbon, B: aliphatic carbon, C: carboxyl moiety, D: alcohol or ether moieties, E: carbonate.

- [1] Y. Kebukawa and G. D. Cody, *Icarus* **248** (2015) 412.
- [2] H. Yabuta *et al.*, *Meteorit. Planet. Sci.* **42** (2007) 37.
- [3] M. Uesugi and A. Nakato, UVSOR activity report (2015)
- [4] N. D. Bassim *et al.*, *J. Microsc.* **245** (2012) 288.
- [5] G. D. Cody *et al.*, *Earth Planet. Sci. Lett.* **272** (2008) 446.

BL4U

Carbon Materials and Alteration Products in Martian Meteorites

H. Suga¹, N. Sago¹, M. Miyahara¹, T. Ohigashi², Y. Inagaki², A. Yamaguchi³ and E. Ohtani⁴

¹Department of Earth and Planetary Systems Science, Graduate School of Science, Hiroshima University, Higashi-Hiroshima 739-8526, Japan

²UVSOR Facility, Institute for Molecular Science, Okazaki 444-8585, Japan

³National Institute of Polar Research, Tokyo 190-8518, Japan

⁴Department of Earth Sciences, Graduate School of Science, Tohoku University, Sendai 980-8578, Japan

It is now widely accepted that water existed on the Mars. Martian surface materials were launched from the Mars by an impact event, and only a few of them were delivered to the Earth, which are so called Martian meteorites. It is expected that one group of Martian meteorite, nakhlite records a water-rock reaction (alteration) occurred on the Mars [e.g., 1]. Iddingsite is one of pervasive alteration textures found in nakhlites. A small amount of carbon materials is accompanied with the iddingsite texture [2]. The constituents, chemical species, and their coordination in the iddingsite textures strongly depend on pH, temperature, rock/water ratio, and pressure during the alteration process. The scrutiny of iddingsite in nakhlites will become a clue for elucidating environment on the Mars during a wet-period. However, the sample volume of nakhlite available for a study is limited because nakhlite is very a precious sample. Iddingsite texture is only about several 10 μm across. Accordingly, we adopted a FIB-assisted site-specific carbon/water-free STXM/NEXAFS technique [3] to investigate iddingsite texture in nakhlite.

Yamato 000593 and Nakhlite samples were prepared for this study. We observed the Yamato 000593 and Nakhlite using a FE-SEM. A laser micro-Raman spectroscopy was employed for phase identification. Several target portions for a STXM analysis were excavated by a FIB technique and became ultra-thin foils. A STXM analysis was conducted at BL4U. Finally, the foils were observed with a FE-STEM.

Both Nakhla and Yamato 000593 consist mainly of augite and minor olivine [(Mg,Fe)₂SiO₄]. FE-SEM observations revealed that iddingsite textures were observed in and around the olivine grains. Based on Raman spectroscopy analysis, the iddingsite textures in the olivine grains mainly appear to consist of a nonstoichiometric distorted olivine-type mineral, laifunite [(Fe²⁺Fe³⁺)₂(SiO₄)₂], which is the alteration product of original olivine. The iddingsite textures around the olivine grains are complex and varied. Silica-rich, sulfur-rich, and chlorine-rich veinlets in addition to laifunite occurred around the olivine grains. Slices for STXM measurements were excavated from these iddingsite textures. Fe- and O-XANES indicate that most iron in original olivine is ferrous (Fe²⁺/Fe³⁺ = 0.72), whereas most iron in laifunite is ferric (Fe²⁺/Fe³⁺ = 0.52). Fe²⁺/Fe³⁺ ratio decreases discontinuously from olivine to laifunite (Fig. 1). Combined FE-SEM, XANES, and STEM

analysis allowed us to follow the alteration sequence from olivine to laifunite for the first time. S-XANES revealed that sulfur in the sulfur-rich veinlet existed as hexavalent rather than zero-valent by comparing with reference materials (sulfur, iron sulfate (iii) hydrate, and iron (II) sulfate heptahydrate). Although Si-XANES was obtained from the silica-rich veinlet, the spectrum was ambiguous (probably due to strong adsorption). Cl-XANES could not be obtained from the Cl-rich veinlet due to lack of an adequate reference material. Alternatively, C- and O-XANES taken showed that the Cl-rich veinlet included both carbon and oxygen, and aromatic hydrocarbons (C=C) was detected. Although we have not completed all measurements, our site-specific STXM/NEXAFS technique is now uncovering complex and varied alteration processes occurred on the early Mars.

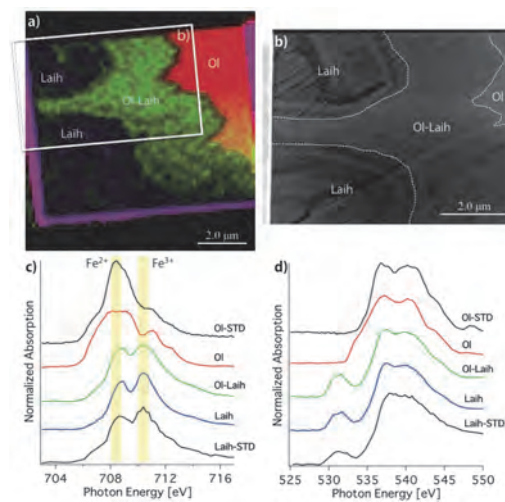


Fig. 1. a) Fe²⁺/Fe³⁺ ratio distribution in iddingsite texture, b) STEM image of a box in a), c) and d) are the Fe- and O-XANES for olivine (Ol), olivine-laifunite intermediate (Ol-Laih), and laifunite (Laih) domains with standard (STD) materials, respectively.

[1] T. Noguchi *et al.*, *J. Geophys. Res.* **114** (2009) E10004.

[2] L. M. White *et al.*, *Astrobiology* **14** (2014) 170.

[3] H. Suga *et al.*, in prep.

BL4U

Chemical Evaluations of Sample Preparation Methods for C-, N-, O-XANES/STXM

Y. Kebukawa¹, E. Uchimura², T. Ohigashi³, Y. Inagaki³ and K. Kobayashi¹

¹ Faculty of Engineering, Yokohama National University, Yokohama 240-8501, Japan

² School of Engineering Science, Yokohama National University, Yokohama 240-8501, Japan

³ UVSOR Synchrotron, Institute for Molecular Science, Okazaki 444-8585, Japan

Carbon, nitrogen, oxygen X-ray absorption near edge structure (XANES) with scanning transmission X-ray microscope (STXM) became a powerful tool for extraterrestrial organic matter analyses in this decade. Some problems may still exist due to small amount of organic matter that usually exists in extraterrestrial samples, such as meteorites, and its susceptibility to damage, degradation and contamination. Here we compared the sample preparation methods for STXM and evaluate whether correct organic chemistry would be reflected and reproduced.

We prepared ~100 nm-thick thin sections of Murchison meteorite and humic acid (IHSS standard Leonardite humic acid, as an analog of organic matter in meteorites) using a focused ion beam (FIB) and an ultramicrotome (UMT) equipped with a diamond knife. For UMT, the sample grains were mixed with sulfur powder and heated to melt the sulfur (~150°C for less than one minute). Solidified sulfur droplet was attached to an epoxy stub. The ultramicrotomed sections were transferred to SiO-coated TEM grids and gently heated until the sulfur sublimed off. C, N, O-XANES spectra were obtained at BL4U, UVSOR.

Figure 1 shows C-XANES spectra of the Murchison and humic acid prepared with UMT and FIB. C-XANES spectra of the Murchison show some differences between UMT and FIB. Ketone C=O appeared only in FIB sample and C-O (alcohol, ether) appeared only in UMT sample. Ketone might be increased due to FIB beam damage, while C-O in UMT sample might be a contamination during sample preparation. Note that the Murchison has some heterogeneity so we examined C-XANES from several different locations. While humic acid prepared in either UMT or FIB showed no significant difference in C-XANES, indicating that slight damage/contamination affects when one intend to detect small amount of organic matter embedded in mineral matrix. Figure 2 shows elemental abundances calculated using computational fit of C-, N-, and O-XANES spectra [1]. The O/C ratio obtained with XANES are underestimated compared to elemental composition data for the humic acid standard provided by International Humic Substances Society (IHSS) [2]. These results indicate that XANES data interpretations must be made with cautions.

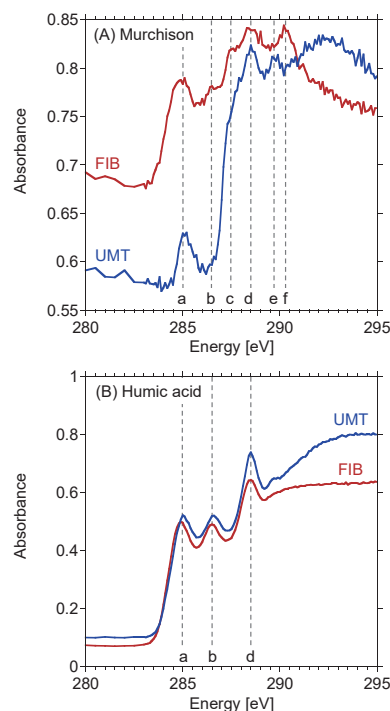


Fig. 1. C-XANES spectra of (A) Murchison and (B) humic acid. Peak assignments [1]; a: 285.0 eV, aromatic C=C, b: 286.5 eV, ketone C=O, c: 287.5 eV, aliphatic C-C, d: 288.5 eV, carboxyl O=C-O, e: 289.7 eV, alcohol, ether C-O, f: 290.3 eV, carbonate CO₃.

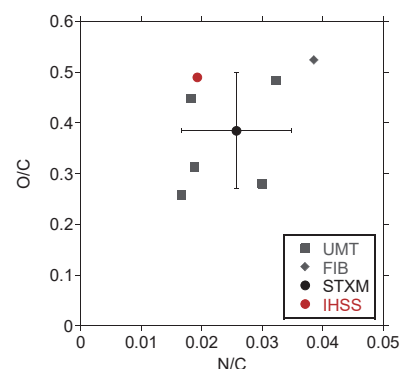


Fig. 2. Atomic N/C versus O/C derived from C-, N-, and O-XANES of humic acid. An average of 5 UMT data points and one FIB data point is plotted in a black circle. IHSS reference data [2] is included in the plot (red circle).

[1] G. D. Cody *et al.*, *Meteorit. Planet. Sci.* **43** (2008) 353.

[2] <http://www.humicsubstances.org>

BL4U

Speciation of Carbon in Prokaryotic Organelles of *Pseudanabaena foetida* (*Phormidium tenue*)

K. Takemoto¹, M. Yoshimura², Y. Inagaki³ and T. Ohigashi³¹Department of Physics, Kansai Medical University, Hirakata 573-1010, Japan²SR center, Ritsumeikan University, Kusatsu 525-8577, Japan³UVSOR Synchrotron, Institute for Molecular Science, Okazaki 444-8585, Japan

Lake Biwa is the most important water reservoir in Kyoto-Osaka-Kobe region in Japan. In 1969, the musty-odor occurred due to sudden propagation of a certain cyanobacterium in Lake Biwa. Since then, the musty-odor problem in Lake Biwa is reported almost every year. The matter of the musty-odor was identified as 2-methylisoborneol (2-MIB) [1]. Although the musty-odor-causing cyanobacterium was reported as *Phormidium tenue* (Menegh.) Gomont, in 2016, the cyanobacterium was proposed as a new species producing 2-MIB: *Pseudanabaena foetida* Niiyama, Tuji *et* Ichise sp. nov. [2]. Now, the study how the microstructure and growth condition are related to the 2-MIB productivity has proceeded. In our previous study based on full field transmission soft X-ray microscope observation, two interesting intracellular structure were observed. One is oxygen-enriched granules and the other is carbon-enriched structures. Oxygen distribution and K-edge XANES spectra were collected on the scanning transmission X-ray microscope (STXM) at UVSOR BL4U [3]. Several oxygen-enriched granules were confirmed. Though the pre-peak intensity of oxygen-enriched granules was smaller than that of cytoplasm, the pre-peak energies were almost similar.

However, the main edge energy of the granule shifted toward lower than that of cytoplasm. In this study, the carbon-enriched structures were examined using STXM.

P. foetida sp. collected from Lake Biwa were subcultured. The culture was maintained on CT medium (pH 8.0) under a 12 h light/12 h dark cycle at 20 °C. The cultures were illuminated with fluorescent lamps, which provided about 20 $\mu\text{mol photons m}^{-2} \text{s}^{-1}$ of photosynthetically active radiation.

Figures 1 a and b show XM images of air-dried *P. foetida* cells. Oxygen was localized around the center of the cells like a belt (Fig. 1a). Since a blank area was seen in the belt-like oxygen localizing area, black arrow, a carbon image was taken at 285 eV (Fig. 1b). At the oxygen blank area, area 1, a structure with high X-ray absorption characteristic was seen. As shown in Fig. 1c, the carbon XANES spectra were similar, but only the spectrum from area 1 showed a peak at 297 eV assigned to potassium, asterisk. It is well known that in bacteria, sodium, potassium, calcium, and magnesium have all been shown to effect cell division [4]. This result suggests that localization of potassium is implicated as the site of regulation of cell division of *P. foetida*.

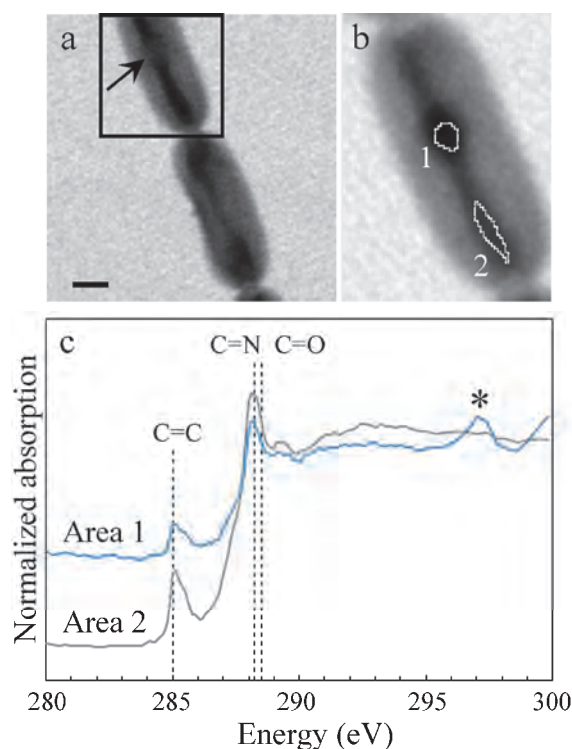


Fig. 1. STXM images of *P. foetida* cell taken at 532 eV (a) and 285 eV (b) and carbon XANES spectra (c). The blue and grey spectra correspond to the area 1 and 2 in (b). The peak around 285 eV, 288.2 eV and 288.5 eV were assigned to C=C, C=N and C=O, respectively. Scale bar is 1 μm .

- [1] M. Yagi *et al.*, Water Sci. Technol. **15** (1983) 311.
 [2] Y. Niiyama *et al.*, Fottea **16** (2016) 1.
 [3] T. Ohigashi *et al.*, J. Phys. Conf. Ser. **463** (2013) 012006.
 [4] L. O. Ingram *et al.*, J. Bacteriol. **125** (1976) 369.

BL6B

Observation of Infinitesimal Optical Isomers in Homochiral Aspartic Acid Films by Infrared MicroMicro-Spectroscopic Imaging

J. Hibi¹, S. Kamei¹ and S. Kimura^{1,2}¹Graduate School of Frontier Biosciences, Osaka University, Suita 565-0871, Japan²Department of Physics, Graduate School of Science, Osaka University, Toyonaka 560-0043, Japan

Proteins, which play an important role in living bodies, are composed of many kinds of amino acids. Among amino acids except for glycine, there are two types of optical isomers, L- and D-types, whose physical and chemical properties are equal to each other, but, most of amino acids in living bodies are L-type. However, in recent years, it has been revealed that L-amino acids change to D-amino acids in proteins by aging and the change from L- to D-type (racemization) is considered to be related to aging diseases such as cataract and Alzheimer's disease. Even among amino acids, racemization of aspartic acid (Asp) is relatively easy to occur in proteins of aged human lens [1]. In crystallin that is a protein in Human lens, for example, the amount of D-Asp increases by aging but is infinitesimal in comparison with L-Asp [1]. To detect the D-Asp as well as D-amino acid in L-type one, special complex techniques are needed, for instance, a special chromatography with asymmetric catalysts, are used at present. In addition, the spatial distribution of D-Asp cannot be detected easily.

To verify whether we can detect infinitesimal D-Asp in the majority of L-Asp and also the spatial distribution, we performed an infrared micro-spectroscopic imaging of aspartic acids thin film.. Thin film samples of L- and D-Asp on potassium bromide (KBr) substrates were fabricated by a vacuum evaporating method. We made two kinds of samples, one is a pure L-Asp film (namely D:0%) and the other contains D-Asp by 1% (namely D:1%). The D:1% thin film of was fabricated by the mixture using a pestle in a mortar beforehand. Infrared micro-spectroscopic imaging (IR imaging) were performed by a reflection mode at BL6B using the infrared microscope (FT/IR 6100 + IRT 7000, JASCO Co., Ltd.) Wavenumber and spatial resolutions were set as 2 cm⁻¹ and 100 μm, respectively. The interval of each step was set to the same as the spatial resolution. The wavenumber range was 600-4000 cm⁻¹.

Figure 1a indicates normalized reflectivity spectra of D:0% and D:1% in the wavenumber range at around 1400 cm⁻¹. The observed peak shifts to the higher wavenumber side by the mixture of D-type. This result suggests that we can detect a tiny amount of D-Asp (1%) mixed in the majority of L-Asp by infrared spectroscopy. To check whether the spatial image of D-Asp can be detected, we measured reflectivity imaging of the sample that contains the D:0% and D:1% areas (Fig. 1b) and obtained the peak wavenumbers at each point by the fitting using the Lorentz model. Figure 1c

shows the spatial distribution of peak wavenumber. Comparing with visible image of Fig. 1b, the border of the areas of D:1% and D:0% can be observed. Therefore, we can conclude that the presence of the tiny amount of D-Asp can be visualized by the IR imaging. Moreover, we can perform the IR imaging with the high spatial resolution and high contrast using infrared synchrotron radiation (IRSR). Therefore, more detailed information will be expected by using IRSR.

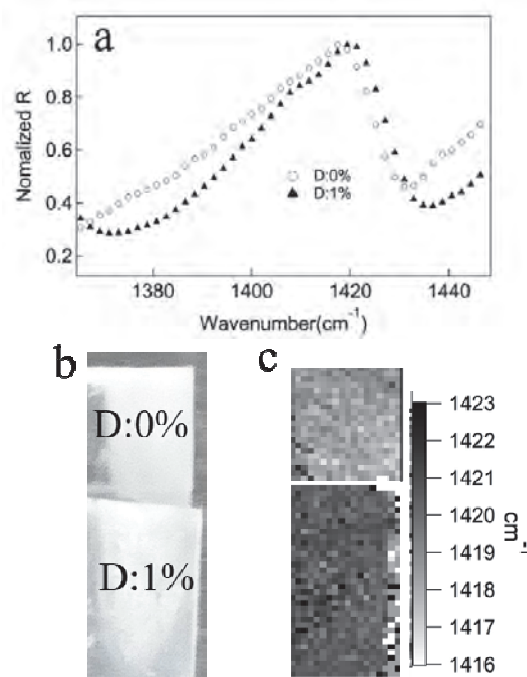


Fig. 1. (a) Normalized reflectivity spectra of thin film samples of pure L-Asp (D:0%) and 1-% D-Asp in L-Asp (D:1%). (b) Photo of the sample (D:0% and D:1% films on KBr). (c) Spatial distribution of peak wavenumber of the sample. The peak position corresponds to that of (a).

[1] N. Fujii *et al.*, Biol. Pharm. Bull. **28** (2005) 1585.

[2] S. Kimura and Y. Ikemoto, Hoshako **18** (2005) 5 [in Japanese].

UVSOR User 9

